

Dynamical imperfections in quantum computers

Paolo Facchi,¹ Simone Montangero,² Rosario Fazio,² and Saverio Pascazio¹

¹*Dipartimento di Fisica, Università di Bari, I-70126 Bari, Italy and INFN, Sezione di Bari, I-70126 Bari, Italy*

²*NEST-INFM & Scuola Normale Superiore, Piazza dei Cavalieri 7, 56126 Pisa, Italy*

(Received 14 July 2004; published 22 June 2005)

We study the effects of dynamical imperfections in quantum computers. By considering an explicit example, we identify different regimes ranging from the low-frequency case, where the imperfections can be considered as static but with renormalized parameters, to the high-frequency fluctuations, where the effects of imperfections are completely wiped out. We generalize our results by proving a theorem on the dynamical evolution of a system in the presence of dynamical perturbations.

DOI: 10.1103/PhysRevA.71.060306

PACS number(s): 03.67.Lx, 03.67.Mn, 03.67.Pp, 05.45.Mt

In any experimental implementation of a quantum information protocol [1] one has to face the presence of errors. The coupling of the quantum computer to the surrounding environment is responsible for decoherence [2], which ultimately degrades the performances of quantum computation. The presence of static imperfections, although not leading to any decoherence, may also be detrimental for quantum computers. For instance, a small inaccuracy in the coupling constants, inducing as a consequence to errors in the quantum gates, can be tolerated only up to a certain threshold [3]. Moreover, the role of static imperfections depends on the regime, chaotic or not, of the system under consideration [3]. The stability of a quantum computation in the presence of static imperfections has been already analyzed both in terms of fidelity [3–5] and entanglement [6].

A strict separation in “static” imperfections and “dynamical” noise may not be always satisfactory. Dynamical noise may be considered at the same level as static imperfections, if its evolution occurs on a scale much larger than the computational time. In Ref. [4] it was suggested that the effects of static imperfections can be more disruptive than noise for quantum computation. In this paper, we intend to explore this problem in more detail. The model we consider, in spite of its simplicity, enables one to grasp the interplay between the different time scales that appear in the problem. We consider each qubit coupled to a stochastic variable that changes in time with a fixed frequency. Below a given threshold (frequency), the errors can be considered as static, and thus can be corrected by using any of the known methods. The difference between the chaotic and the other dynamical regimes, found for static imperfections, holds also in the quasistatic case. We then generalize our results, by proving a theorem that states that, under general assumptions, in a perturbed system, unitary dynamical errors are averaged to zero in probability. Our results can be relevant in the context of the strategies that have been proposed during the last few years in order to suppress decoherence [7].

Model. Following [3,4], we model a quantum computer as a lattice of interacting spins (qubits). Due to the imperfections, the couplings between the qubits and with an external field are both random and fluctuate in time. We consider n qubits on a two-dimensional lattice, described by the Hamiltonian

$$H(t) = \sum_{j=1}^n [\Delta_0 + \delta_j(t)] \sigma_z^{(j)} + \sum_{\langle i,j \rangle} J_{ij}(t) \sigma_x^{(i)} \sigma_x^{(j)}, \quad (1)$$

where the $\sigma_\alpha^{(i)}$ s ($\alpha=x,y,z$) are the Pauli matrices for qubit i and the second sum runs over the nearest-neighbor pairs. The energy spacing between the up and down states of a qubit is $\Delta_0 + \delta_j(t)$, where the $\delta_j(t)$'s are uniformly distributed in the interval $[-\delta/2, \delta/2]$ and the $J_{ij}(t)$'s in the interval $[-J, J]$ (zero means and variances $\delta^2\sigma^2$ and $4J^2\sigma^2$, respectively, with $\sigma^2=1/12$). We model the dynamical noise by supposing that both $\delta_j(t)$ and $J_{ij}(t)$ change randomly after a time interval τ . Within the time interval they are constant.

For $J=\delta=0$ the spectrum of the Hamiltonian is composed of $n+1$ degenerate levels, with interlevel spacing $2\Delta_0$, corresponding to the energy required to flip a single qubit. We study the case $\delta, J \ll \Delta_0$, in which the degeneracies are resolved and the spectrum is composed by $n+1$ bands. In this limit the coupling between different bands is very weak and each state is effectively coupled to $O(n)$ other states inside the band. We assume free boundary conditions and express all the energy in units Δ_0 ($\hbar=1$).

In the following we analyze the behavior of the fidelity [8] and the error

$$F(t) \equiv |\langle \Psi | U(t) | \Psi \rangle|^2, \quad E_t = -\ln F, \quad (2)$$

starting from an initial state $|\Psi\rangle$, which is an eigenstate of $\sigma_z^{(j)}$ ($j=1, \dots, n$), $U(t)$ being the unitary evolution generated by (1). We concentrate on the central band of zero total magnetization, characterized by the highest density of states, and for which one expects the effect of noise to be most pronounced.

Results. The decay of fidelity due to *static* imperfections (constant δ 's and J 's) is displayed in the inset of Fig. 1. System (1) is characterized by two distinct dynamical regimes: the Fermi golden rule (FGR) ($J < J_c$) and the ergodic regime ($J > J_c$), where $J_c \sim \delta/n$ [3,6]. The FGR holds below threshold (weak coupling) and is characterized by a Lorentzian local density of states with a width $\Gamma_{\text{FGR}} \propto J^2 \rho_{\text{eff}}$, where $\rho_{\text{eff}} \propto 1/\delta$ is the density of states directly coupled to the initial state. The ergodic regime takes place when all the levels inside the band participate to the dynamics: the local density of states has a Gaussian shape with variance $\Gamma_{\text{erg}}^2 \propto J^2$ and

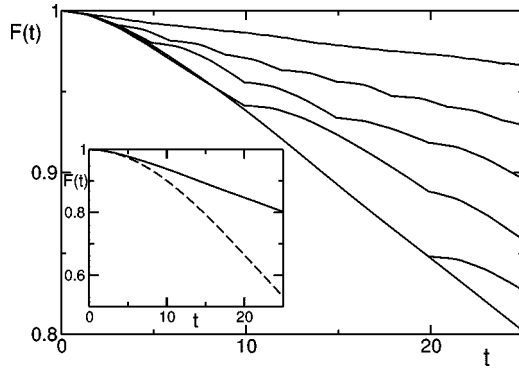


FIG. 1. Fidelity as a function of time for $n=14$ qubits in the FGR regime ($J=2 \times 10^{-2}$, $\delta=4 \times 10^{-1}$) and from top to bottom $\tau=1, 3, 5, 10, 20, 25$ (static imperfections). Inset: Fidelity as a function of time in the ergodic ($J=\delta=2 \times 10^{-2}$, dashed line), and in the FGR regime (full line): note the (common) short-time quadratic law.

coincides with the density of states. The fidelity decay is the Fourier transform of the local density of states [9] and always starts with a quadratic law (see inset Fig. 1), independently of the regime. After this initial common regime, fidelity follows an exponential or a Gaussian decay with characteristic rates $\Gamma_{\text{FGR}}, \Gamma_{\text{erg}}$, respectively [3]. In the strong-coupling (ergodic) regime the decay of fidelity is the result of many different transitions [9]: $F(t) \approx \prod_{(i,j)} \cos^2(J_{ij}t)$, yielding the above-mentioned Gaussian decay $F(t) \approx e^{-J^2 m^2 t}$.

This was the static picture. In the case of *dynamical* imperfections, different regimes emerge as a function of the frequency $1/\tau$. Below a critical time scale τ_c the different behavior due to the ergodic and FGR regimes cannot be resolved anymore. This can be clearly seen in Figs. 1 and 2. An additional (smoother) crossover appears at an even higher frequency $1/\tau_p$ (Fig. 2) when the noise frequency become comparable with the single qubit natural frequency ($\sim \Delta_0$). The error $E_t(\tau)$ at (fixed) time t tends to vanish as τ decreases. From this perspective the overall trend is similar to

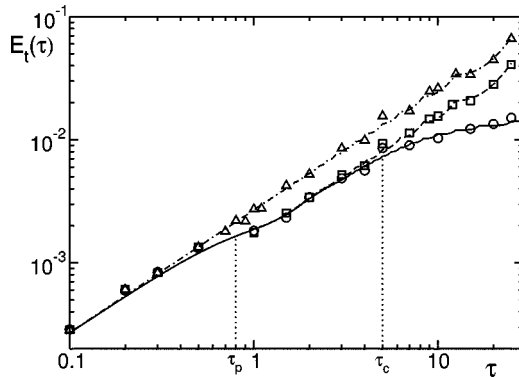


FIG. 2. Error E as a function of τ for $t=25$, $n=10$, $J=5 \times 10^{-3}$, in the ergodic regime $\delta=5 \times 10^{-3}$, $n_{\uparrow\downarrow}=8$ (squares), $n_{\uparrow\downarrow}=13$ (triangles), and in the FGR regime $\delta=3 \times 10^{-1}$ (circles). The fits are given by Eqs. (3), (6), and (7), with $\sigma^2=1/12$, $n_c=13$, $\Delta_0=1$, and $(n_{\uparrow\downarrow}, n_{\uparrow\uparrow})$ equal to (8, 5) (dashed), (13, 0) (dot-dashed). The transition at τ_c is shown only in the former case. All the errors scale as J^2 (data not shown).

the motional narrowing in nuclear magnetic resonance [10]. Most interesting in what we discuss is the emergence of different dynamical regimes as a function of τ .

An explicit calculation of the error to order J^2 yields

$$E_t(\tau) = 4J^2 \sigma^2 [Ng(\tau) + g(\Delta t)], \quad (3)$$

where $t=N\tau+\Delta t$, with N integer, $0 \leq \Delta t < \tau$, and

$$\begin{aligned} g(\tau) &= 2 \int_0^\tau ds \int_0^s du \operatorname{sinc}^2(\delta u) [n_{\uparrow\downarrow} + n_{\uparrow\uparrow} \cos(4\Delta_0 u)] \\ &= n_{\uparrow\downarrow} f(\delta\tau)/\delta^2 + n_{\uparrow\uparrow} D_{\delta\tau} f(2\Delta_0\tau)/\delta^2, \end{aligned} \quad (4)$$

$n_{\uparrow\downarrow}(n_{\uparrow\uparrow})$ being the number of nearest-neighbor parallel (antiparallel) pairs in the initial state, $\operatorname{sinc}(x)=(\sin x)/x$, $D_y f(x)=[f(x+y)-2f(x)+f(x-y)]/2$ and

$$f(x) = \operatorname{Ci}(2x) + 2x \operatorname{Si}(2x) - \ln(2x) + \cos(2x) - \gamma - 1, \quad (5)$$

$\operatorname{Ci}(z)$, $\operatorname{Si}(z)$, and $\gamma \approx 0.577$ being the cosine and sine integral functions, and Euler's constant, respectively. Note that, due to the convexity of $g(\tau)$, the error $E_t(\tau) \leq 4J^2 \sigma^2 t g(\tau)/\tau$, the inequality is saturated when $t/\tau=N$, thus providing a simple interpolation of (3). The function $g(\tau)$ can be approximated in several important limits. For $\tau\delta \ll 1$

$$g(\tau) \approx \tau^2 [n_{\uparrow\downarrow} + n_{\uparrow\uparrow} \operatorname{sinc}^2(2\Delta_0\tau)], \quad (6)$$

which yields $g(\tau) \approx n_c \tau^2$ for $\tau \leq \tau_p = \pi/4\Delta_0$ and $g(\tau) \approx n_{\uparrow\downarrow} \tau^2$ (ergodic regime) for $\tau \geq \tau_p$ (see Fig. 2), where the total number of links $n_c = n_{\uparrow\downarrow} + n_{\uparrow\uparrow}$ [11]. On the other hand, when $\tau\delta \gg 1$, by plugging the asymptotic expansion of (5) into (4), one gets

$$g(\tau) \approx \frac{n_{\uparrow\downarrow}}{\delta^2} [\pi\delta\tau - \ln(2\delta\tau) - \gamma - 1]. \quad (7)$$

Note that the limit $\tau\delta \gg 1$ is within the range of applicability of Eq. (3), only in the FGR regime.

Substituting these approximate expressions in Eq. (3), the error at a fixed time t for different τ values scales like

$$E_t(\tau) \approx 4J^2 \sigma^2 t \begin{cases} n_c \tau & \tau < \tau_p & (\text{all regimes}) \\ n_{\uparrow\downarrow} \tau & \tau_p < \tau < \tau_c & (\text{all regimes}) \\ n_{\uparrow\downarrow} \tau & \tau > \tau_c, J = \delta & (\text{ergodic}) \\ n_{\uparrow\downarrow} \pi/\delta & \tau > \tau_c, J < \delta/n & (\text{FGR}). \end{cases} \quad (8)$$

In Fig. 2 we show the scaling of $E_t(\tau)$ with τ for different values of δ . For the ergodic regime we choose $J=\delta$, while the FGR is characterized by $J \ll \delta$. As $\tau < \tau_c$ the two distinct ergodic and FGR behaviors of the static case (compared in Fig. 2 only for the sets with $n_{\uparrow\downarrow}=8$) are not resolved. Equations (6) and (7), plotted in Fig. 2, are in excellent agreement with the numerical results. The additional kink at $\tau \approx \tau_p = \pi/4\Delta_0$ sets in when single spin dynamics starts to play a role. We also checked that τ_p is independent on J and δ , in agreement with Eq. (6). The transition at $\tau = \tau_c$ is striking and occurs when the error starts deviating from the linear behavior given by Eq. (8). In fact, the crossover between the two regimes could be defined by equating the third and the fourth line of (8), that is for $\tau = \pi/\delta$, which for $\delta=0.3$ would

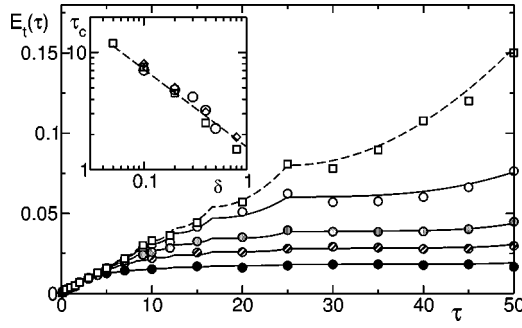


FIG. 3. Error at time $t=50$, for $n=10$, $J=5 \times 10^{-3}$ and different δ values. The squares represent the ergodic regime $\delta=J$. The FGR regime is plotted for $\delta=1, 2, 3, 5 \times 10^{-1}$ (empty, pointed, dashed, full circles, respectively). Inset: τ_c as a function of δ for $n=10, 12, 14$ (circles, squares, and diamonds, respectively). The dashed line is proportional to $\delta^{-2/3}$, in agreement with Eq. (10).

give $\tau \approx 10.5$. However, since the saturation value $E_t(\tau) = \Gamma_{\text{FGR}} t = 4J^2 \sigma^2 n_{\uparrow\downarrow} \pi t / \delta$ given by Eq. (8) is reached only for $\delta \tau \gg 1$ and since the transition is sharp, a much more accurate way to define τ_c is by looking at the point for which the deviation from the linear behavior [third line in Eq. (8)] becomes apparent. To this purpose we keep the next-leading correction to Eq. (6) and approximate $\text{sinc}^2(\delta u) \approx 1 - (\delta u)^2/3$ (for $\tau \lesssim 1/\delta$) in the integral (4). For $\tau \gtrsim \tau_p$ we obtain

$$g(\tau) \approx \frac{n_{\uparrow\downarrow}}{\delta^2} \left[(\delta\tau)^2 - \frac{(\delta\tau)^4}{18} \right]. \quad (9)$$

If the plot resolution in Fig. 2 is some fraction ε of the total vertical range $4J^2 \sigma^2 n_{\uparrow\downarrow} t^2$, the error curve starts deviating from the linear behavior when $(t/\tau)(\delta\tau)^4/(18\delta^2) \approx \varepsilon t^2$, i.e.,

$$\tau_c = \frac{(18\varepsilon t)^{1/3}}{\delta^{2/3}}, \quad (10)$$

which for $t=25$, $\delta=0.3$, and $\varepsilon=1/40$ yields $\tau_c=5$, in full agreement with Fig. 2. In Fig. 3 we show the error $E_t(\tau)$ with fixed J and different δ values. The scaling of the critical threshold τ_c is clearly visible. We also checked that τ_c does not depend on J (data not shown). The inset of Fig. 3 shows the dependence of τ_c as a function of δ , confirming the prediction (10).

Theorem. After having presented the overall picture of dynamical imperfections on the fidelity of computation, we complete our analysis and set up a general framework to consider the effect of a time-dependent noise on the evolution of a quantum system

$$H(t) = H_0 + \xi(t)V, \quad (11)$$

where H_0 is time independent and $H(t)$ varies with a given characteristic time τ , according to the stochastic process with independent increments $\xi(t) = \sum_{k=1}^N \chi_{[k\tau-\tau, k\tau)}(t) \xi_k$, where χ_A is the characteristic function of the set A and $\{\xi_k\}_k$ are independent and identically distributed random variables, with expectations $E[\xi_k]=0$, $\text{Var}[\xi_k]=E[\xi_k^2]=\sigma^2 < \infty$. The time evolution operator over the total time $t=\tau N$ is given by

$$U_N(t) = \prod_{k=1}^{t/\tau} \exp[-i(H_0 + \xi_k V)\tau], \quad (12)$$

where a time-ordered product is understood, with earlier times (lower k) at the right. Let us assume, for simplicity, that H_0 and V are bounded operators, so that $U(t)$ is a norm-continuous one-parameter group of unitaries and all our subsequent estimates are valid in norm. We are interested in the existence and form of the limiting time evolution operator $U_N(t)$ for $N \rightarrow \infty$. When expanding the product, one finds that the term independent of t is 1, while the term proportional to t reads $-iH_0 t - iVt \sum_{k=1}^N \xi_k / N$. Now, according to the weak law of large numbers [12], $P\text{-}\lim_{N \rightarrow \infty} \sum_{k=1}^N \xi_k / N = E[\xi_k] = 0$, for we assumed $E[\xi_k^2] = \sigma^2 < \infty$, and the limit is taken in probability. Therefore, for $N \rightarrow \infty$

$$1 - iH_0 t - iVt \frac{1}{N} \sum_{k=1}^N \xi_k \xrightarrow{P} 1 - iH_0 t. \quad (13)$$

Analogously, by using the weak law of large numbers, one can prove that all higher powers of Vt vanish in the limit, thus obtaining

$$U(t) \equiv P\text{-}\lim_{N \rightarrow \infty} U_N(t) = \exp(-iH_0 t), \quad (14)$$

in the following sense

$$\lim_{N \rightarrow \infty} P(\|U_N(t) - \exp(-iH_0 t)\| \geq \varepsilon) = 0, \quad (15)$$

uniformly in each compact time interval. If the term $\xi(t)V$ is viewed as exemplifying the effect of (dynamical) error-inducing disturbances, the above result physically implies that the effects of the errors are wiped out if their characteristic frequency τ^{-1} is sufficiently fast. This defines the purely dynamical regime.

Another viewpoint can also be adopted, that is somewhat complementary to the above one. Given a characteristic frequency of the noise, it is possible to establish an *effective* value of the strength of the imperfections so that the above result holds (approximately). In this sense, a natural question is what happens for large but *finite* N . This question can be answered by remembering that under the same hypotheses, according to the central limit theorem, the limiting random variable $\eta = \lim_{N \rightarrow \infty} \sum_{k=1}^N \xi_k / \sqrt{N}$ exists and is Gaussian with mean $E[\eta]=0$ and variance $E[\eta^2]=\sigma^2$, namely it is distributed like $f(\eta) = (2\pi\sigma^2)^{-1/2} \exp(-\eta^2/2\sigma^2)$. Thus, by following the same steps that led to (14), we find that for $N \gg 1$

$$U_N(t) \sim \exp(-iH_0 t) \exp(-i\eta V t / \sqrt{N}). \quad (16)$$

Equation (16) implies then that for *fixed* τ , the system “feels” an effective interaction strength $\epsilon_{\text{eff}} = \sigma \|V\| / \sqrt{N} \propto \sigma \|V\| / \sqrt{\tau}$.

For intermediate values of N , Eq. (16) is no longer valid, because it hinges upon the commutativity of H_0 and V . However, by assuming that $V \ll H_0$ (e.g., in norm), a straightforward expansion shows that the perturbation V is replaced by

$$\bar{V}(\tau) = \frac{1}{\tau} \int_0^\tau dt e^{iH_0 t} V e^{-iH_0 t}, \quad (17)$$

so that, for $\tau \|H_0\| \geq 2\pi$, the effective perturbation becomes

$$\bar{V}(\tau) \rightarrow V_Z = \sum_k P_k V P_k, \quad (18)$$

where P_k are the eigenprojections of H_0 ($H_0 = \sum \lambda_k P_k$). This phenomenon is reminiscent of the quantum Zeno subspaces [13].

The generalization of the above results to a Hamiltonian with a family of independent stochastic processes with zero mean and finite variances is straightforward. This is the case of the Hamiltonian (1), which reads

$$H(t) = H_0 + \delta \xi_0(t) \cdot \mathbf{V}_0 + 2J \xi(t) \cdot \mathbf{V}, \quad (19)$$

where $H_0 = \sum_j \Delta_0 \sigma_z^{(j)}$, $(\mathbf{V}_0)_j = \sigma_z^{(j)}$, $(\mathbf{V})_{ij} = \sigma_x^{(i)} \sigma_x^{(j)}$, and $\xi_{0j} = (\xi_0)_j$ and $\xi_{ij} = (\xi)_{ij}$ ($i, j = 1, \dots, n$) are independent random variables uniformly distributed in the interval $[-1/2, 1/2]$.

We can then reinterpret our previous results in the light of the above theorem, by applying the static results [9], outlined before Eq. (3) to the (static) evolution with renormalized couplings (16) (with $\eta V \rightarrow \boldsymbol{\eta} \cdot \mathbf{V}$). Thus, independently of the interaction strength and the correspondent dynamical regime, for sufficiently large N (or small $\tau = t/N$), by expanding (16) to $O(1/N)$, one finds a quadratic decay law

$$E_t(\tau) \sim \frac{1}{N} \frac{t^2}{\tau_Z^2} = \frac{t}{\tau_Z^2} \tau \quad (\tau < \tau_p), \quad (20)$$

where $\tau_Z^{-2} = 4J^2 \langle \Psi | (\boldsymbol{\eta} \cdot \mathbf{V})^2 | \Psi \rangle = 4J^2 n_c \sigma^2$ and $\tau_p \simeq \Delta_0^{-1}$ [the H_0 time scale, see (17)]. On the other hand, for smaller N , i.e., $\tau > \tau_p$, the effective interaction (18) is given by $(\mathbf{V}_Z)_{ij} = \sigma_+^{(i)} \sigma_-^{(j)} + \sigma_-^{(i)} \sigma_+^{(j)}$, whence

$$E_t(\tau) \sim \frac{1}{N} \Gamma_{\text{erg}}^2 t^2 = \Gamma_{\text{erg}}^2 t \tau \quad (\tau > \tau_p), \quad (21)$$

where $\Gamma_{\text{erg}}^2 = 4J^2 \langle \Psi | (\boldsymbol{\eta} \cdot \mathbf{V}_Z)^2 | \Psi \rangle = 4J^2 n_{\uparrow\downarrow} \sigma^2$. Therefore, we recover the linear growth of the error (with the correct coefficients), that describes both regimes up to τ_c in Eq. (8).

Conclusions. We studied the effects of dynamical imperfections on a quantum computer model, depending on the frequency of the external noise. Below a frequency threshold, imperfections can be considered static, although with renormalized parameters, and one observes two different dynamical regimes. Above this threshold these regimes become unresolved. These results are independent of the form and the size of the quantum computer. They remain valid under quite general conditions on the system Hamiltonian, allowing a more general application of these findings.

Our results show that it is crucial to optimize the computing time scale, by choosing it between the two competing types of noise (static and dynamic). In turn, this suggests strategies to develop general error correcting techniques.

This work was supported by the European Community under Contracts IST-SQUBIT, IST-SQUBIT2, and RTN-Nanoscale Dynamics.

-
- [1] M. A. Nielsen and I. L. Chuang, *Quantum Computation and Quantum Information* (Cambridge University Press, 2000).
- [2] I. L. Chuang, R. Laflamme, P. W. Shor, and W. H. Zurek, *Science* **270**, 1635 (1995).
- [3] B. Georgeot and D. L. Shepelyansky, *Phys. Rev. E* **62**, 3504 (2000); **62**, 6366 (2000).
- [4] G. Benenti, G. Casati, S. Montangero, and D. L. Shepelyansky, *Phys. Rev. Lett.* **87**, 227901 (2001).
- [5] C. Miquel, J. P. Paz, and W. H. Zurek, *Phys. Rev. Lett.* **78**, 3971 (1997).
- [6] S. Montangero, G. Benenti, and R. Fazio, *Phys. Rev. Lett.* **91**, 187901 (2003).
- [7] A. Ekert and C. Macchiavello, *Acta Phys. Pol. A* **93**, 63 (1998); quant-ph/9904070.
- [8] A. Peres, *Phys. Rev. A* **30**, 1610 (1984).
- [9] V. V. Flambaum, *Aust. J. Phys.* **53**, N4 (2000).
- [10] C. P. Slichter, *Principles of Magnetic Resonance*, Springer Series in Solid-State Sciences, Vol. 1 (Springer, Berlin, 1990).
- [11] Unlike $n_{\uparrow\downarrow}$ and $n_{\uparrow\uparrow}$, n_c does not depend on the initial state $|\Psi\rangle$.
- [12] W. Feller, *Probability Theory and its Applications*, (John Wiley, New York, 1971), Vol. II.
- [13] P. Facchi and S. Pascazio, *Phys. Rev. Lett.* **89**, 080401 (2002).